UCLA
UCLA Electronic Theses and Dissertations

Title
Perivascular Stem Cells Induce Paracrine-mediated Osteogenesis via Upregulation of Secreted Wnt-related Proteins

Permalink
https://escholarship.org/uc/item/60w8w62m

Author
Asatrian, Gregory

Publication Date
2018

Peer reviewed|Thesis/dissertation

eScholarship.org Powered by the California Digital Library
University of California

UNIVERSITY OF CALIFORNIA

Los Angeles

Perivascular Stem Cells Induce Paracrine-mediated Osteogenesis via Upregulation of Secreted Wnt-related Proteins

A thesis submitted in partial satisfaction of the

requirements for the degree Master of Science

in Oral Biology

by

Gregory Asatrian

2018

ABSTRACT OF THE THESIS

Perivascular Stem Cells Induce Paracrine-mediated Osteogenesis

via Upregulation of Secretory Wnt-related Proteins

by

Gregory Asatrian

Master of Science in Oral Biology

University of California, Los Angeles, 2018

Professor Kang Ting, Chair

With an increase in the number of annual craniomaxillofacial orthopaedic procedures being performed, and an understanding of the drawbacks of autologous bone grafting, the bone graft substitute market is burgeoning. Several bone graft alternatives, including, FDA-approved osteogenic molecule, Bone Morphogenetic Protein-2 have shown promise in promoting large volumes of *de novo* bone formation, however are ladened with several adverse effects, hampering their clinical application. Perivascular Stem Cells (PSC) are a prospectively purified mesenchymal stem cell population isolated from adipose tissue by fluorescent-activated cell sorting (FACS), and have previously been shown to induce robust bone formation in small and large animal models. Herein, by utilizing species-specific MHC immunohistochemistry, we demonstrated that PSC elicit their osteogenic effect primarily via a paracrine-mediate mechanism. Subsequently, after resolving that PSC mediate host mesenchymal stem cells, via the secretion of pro-osteogenic

molecules, RNA sequencing was performed to compare PSC with their unpurified predecessor, stromal vascular fraction (SVF). It was observed that Wnt-related secretory molecules, WISP-1 and Wnt16 were upregulated in PSC by 72- and 21- fold, respectively, when compared to SVF. Gain-of-function assays for these two secretory molecules revealed a significant increase in osteogenic markers, whereby a significant decrease in osteogenic markers was observed when WISP-1 or Wnt16 were knocked-down in PSC. Wnt16 was observed to indeed be a mixed ligand and demonstrate activation of both the canonical and noncanonical Wnt pathways. In aggregate, these data demonstrate that PSC promote osteogenesis via a primarily paracrine-mediate secretion of pro-osteogenic molecules, of which WISP-1 and Wnt16 are highly upregulated and play a functional and necessary role in PSC osteogenesis.

The thesis of Gregory Asatrian is approved.

Diana V Messadi

Flavia Queiroz de mo Pirih

Kang Ting, Committee Chair

University of California, Los Angeles

2018

TABLE OF CONTENTS

ACKNOWLEDGEMENTS vi

SIGNIFICANCE STATEMENT Pg. 1

INTRODUCTION Pg. 1

RESULTS

Direct Differentiation vs Paracrine-Mediated Recruitment of Osteoprogenitor Cells Pg. 5

Activation of Wnt signaling during hPSC Osteogenic Differentiation Pg. 6

WISP-1 and Wnt16 transcripts are upregulated in PSC Pg. 6

Role of WISP-1 in PSC osteogenesis Pg. 7

Role of Wnt16 in PSC osteogenesis Pg. 8

DISCUSSION Pg. 10

CONCLUSION & FUTURE DIRECTION Pg. 12

MATERIALS & METHODS Pg. 13

FIGURES Pg. 20

Figure 1. Isolation Protocol of PSC Pg. 20

Figure 2. Osteoprogenitor origin of newly formed bone cells Pg. 21

Figure 3. Regulation of Wnt signaling during hPSC osteogenic differentiation. Pg. 22

Figure 4. WISP-1 upregulation increases osteogenic differentiation. Pg. 23

Figure 5. *WISP-1* downregulation inhibits osteogenic differentiation Pg. 24

Figure 6. WNT16 and Wnt signaling Pg. 25

Figure 7. WNT16 downregulation inhibits osteogenic differentiation Pg. 26

Figure 8. Schematic representation of hypothesized role of WNT16 & WISP-1. Pg. 27

WORS CITED Pg. 28

ACKNOWLEDGEMENTS

I would like to thank Drs. Kang Ting and Aaron W. James, my mentors, for their continual support and guidance during my BS degree, DDS program and my MS program during orthodontic residency. I am grateful for the opportunity to develop and explore this interesting project over the past 6 years. Their patience, guidance, work ethic, passion, and enthusiasm in research are the driving forces behind this thesis work.

I am thankful for Mr. Matthew Dingman at the Oral Biology department for his assistance in resolving administrative difficulties.

Lastly, I want to thank all the current and past members of Ting Lab for their support and contributions to this project.

This thesis, in part, is adapted from material published in Stem Cells Translational Medicine, published in October, 2014 Vol. 3, 1231-41, and Tissue Engineering, published in January, 2018 Vol. 24, 68-80 with appropriate permissions. The thesis author was also an author of these papers.

Significance Statement

With an increase in the number craniomaxillofacial orthopaedic procedures being performed per annum, and the improvements in the scientific and medical understanding of the drawbacks of autologous bone grafting, the bone graft substitute market is burgeoning. Perivascular Stem Cells (PSC) are a novel, prospectively purified, autologous mesenchymal stem cell population isolated from adipose tissue by fluorescent-activated cell sorting (FACS). Our previous studies have demonstrated that PSC induce robust bone formation in large and small animal models. Until present, a paucity existed regarding the underlying mechanism by which this improved bone formation occurred. Herein, we demonstrate the, primarily, paracrine-mediated osteogenic effect of PSC, via upregulation of secretory molecules WISP-1 and Wnt16, and their downstream canonical and noncanonical Wnt pathway activations. By understanding the mechanism by which PSC mediate bone formation, we can optimize and safely transition these findings to future craniofacial patient care.

Introduction

With over 2.2 million surgeries performed annually, non-healing skeletal defects are addressed in the diverse fields of orthopedic, plastic, and oral surgery [1, 2]. Several modalities of bone regeneration are present in the surgeons' armamentarium, however, most are ladened with significant disadvantages, hampering their clinical application. Autologous bone grafting, frequently isolated from the iliac crest, is still the gold standard for grafting[3], however is encumbered by several significant draw backs including donor site morbidity[4-6], associated complications from an increased operating time and additional surgical site, and a finite autologous supply.

Due to these limitations, investigators sought alternative bone graft substitutes, including, but not limited to, one of the most commonly studied and utilized growth factor, Bone Morphogenetic Protein (BMP)-2. BMP-2 is indeed a U.S. Food and Drug Administration (FDA)-approved osteoinductive growth factor, and has repeatedly been shown to induce robust and abundant bone formation[7, 8]. Current studies and clinical correlates, however, have demonstrated the species-specific dosing response with BMP-2, and a necessary increase in dose concentration with increasing phylogenetic complexity[9]. With this necessary increase in clinical concentration, BMP-2 was observed and confirmed to elicit a number of adverse effects including heterotopic bone formation[10-15], late-osteoclast activation[16-18], cystic bone formation [18-20], and post-operative inflammation[21-24].

Another alternative to bone grafting was the utilization of autologous mesenchymal stem cell (MSC). MSC can accelerate bone regeneration by several mechanisms, including direct bone formation, recruitment and activation of osteoprogenitor cells, immunomodulation, and the promotion of vascularization to the site of implantation [25]. Such mesenchymal stem cells can be harvested from various loci and isolated by several modalities, each of which have several positives attributes, but, again, are outweighed by significant drawbacks (reviewed by Asatrian, *et al* [26]).

The most frequently studied are those MSC isolated from the bone marrow, BMSC[27-29]. BMSC, although possess multi-lineage potential, including potent osteogenic potential[30-32], possess similar drawbacks as autologous bone isolation from the iliac crest, including morbidity and complications of isolation from the hip[33]. Furthermore, BMSC are limited in supply and require several passages of *in vitro* expansion[34], which reduces cellular activity and increases risk of mutations and corresponding immunogenic response[35, 36].

Another site of MSC isolation that was discovered in 2001 by Zuk *et al*, was adipose tissue[37]. Adipose-derived stem cells or stromal cells (ASC) have been studied extensively since their advent due to their abundance in supply and relative ease if harvest via routine liposuction procedures. Subsequent to harvest, lipoaspirates are immediately treated with collagenase, yielding a mixed cell homogenate termed the stromal vascular fraction (SVF). This SVF contains ASC in addition to a mixed population of endothelial, hematopoetic and stromal cells [38, 39]. Purification markers vary from study to study; however, most investigators agree to isolate ASC from SVF via expression of cell markers CD73, CD90, CD44, and CD9[40]. Despite the fact that ASC have been validated to possess consistent osteogenic potential[41-43], ASC still contain significant drawbacks that hinder their clinical application[26]. For instance, much like in BMSC, ASC require *in vitro* cultivation which has been previously been observed to decrease stemness, self-renewal, and multipotency[44]. In select cases, culture of ASC has been observed to result in genomic instability and in-turn malignant transformation[45]. With these significant drawbacks present in BMSC, ASC, and other stem cell populations that were not highlighted herein, there exists a clinical need for a reliable and abundant source of MSC that do not require an extensive isolation protocol.

Perivascular stem cells (PSC) are a homogenous stem cell population that are isolated utilizing fluorescence-activated cell sorting (FACS) from the aforementioned stromal vascular fraction (SVF), a collagenase-treated lipoaspirate (isolation procedure outlined in Figure 1). What differentiates PSC from ASC (adipose-derived stem cells) is the fact that these cells are identified by their cell surface markers using FACS and include pericytes from microvessels and capillaries (which are CD34-, CD146+, CD45-), and adventitial cells from larger arteries and veins (which are CD34+, CD146-, CD45-)[46]. This isolation protocol ensures minimal manipulation and

passages *in vitro*, decreasing the risk of mutation and genetic instability. The composition of pericytes and adventitial cells together, termed PSC, exhibit characteristic surface markers of multilineage potential that has been previously demonstrated in various studies by our group [47-51].

The osteogenic potential of PSC have extensively been verified in several small and large animal studies. First, human adipose-derived PSC were shown to promote bone formation in an ectopic muscle pouch-implantation model, far superior to that of patient-matched, SVF[52, 53]. This increase in osteogenic potential was paralleled with an increase in vascular infiltration[54]. In a subsequent study, PSC, from various patient demographics (gender, age, body mass index(BMI)), were observed to successfully recover mice that were afflicted with a critical-size calvarial defect. As such, it was concluded that PSC possess immense osteogenic potential, irrespective of patient age, gender or BMI[55]. Contingent on these findings, a study was performed to evaluate the dose-dependent effect of human PSC (hPSC) implantation in athymic rats and the success on cervical spinal fusion. It was observed that although all samples treated with hPSC, irrespective of dose, were capable of inducing successful boney bridging, animals treated with a higher concentration of hPSC were observed to possess more bone and of higher density[56]. Importantly, no pathologic findings were observed in any samples in the aforementioned studies.

The mechanism by which PSC induced bone formation, however remains largely unelucidated. To investigate whether the bone formed was by direct differentiate of PSC, much like most MSC, or via recruitment of host osteoprogenitor cells, human PSC were implanted in athymic rats and the newly formed bone was assayed for expression human and/or rat major histocompatibility complex (MHC). Subsequently, RNA sequencing (RNASeq) was performed to assess differential expression of secreted Wnt-related molecules between PSC and unpurified SVF. Loss of function and gain of function assays were next performed to further understand the

mechanism by which PSC induce optimized bone formation. In aggregate, our findings suggest that perivascular stem cells are a potent autologous stem cell population that are ample in supply, capable of promoting robust bone formation via, primarily paracrine-mediated, osteoprogenitor recruitment by means of Wnt-related secretory molecules, WISP1 and Wnt16.

Results

Direct Differentiation vs Paracrine-Mediated Recruitment of Osteoprogenitor Cells

As it has been well documented that PSC harness the potential to induce bone formation in several loci and models, we first sought to investigate whether this bone formation was primarily through direct differentiation of implanted PSC or through recruitment of host mesenchymal stem cells. To answer this preliminary question, athymic rats underwent spinal fusion procedure whereby they were implanted with increasing doses of patient-matched human PSC (hPSC). Sections of the boney bridges were stained using immunohistochemistry for anti-human MHC and anti-rat MHC to assess whether the newly formed bone was of donor- or host- origin (Figure 2A). Qualitative observation of low magnification sections revealed an increased intensity stain for host (rMHC-positive) cells, both in the osteocytes found in the newly formed bone, as well as the bone-lining osteoblasts when compared to donor (hMHC-positive) cells. As anticipated, with the increasing dose of human PSC, a correlate existed with an increased number of human-derived osteoblasts (Figure 2B). Of interest, however, was the significantly higher amount of host (rMHC+) bone-lining osteoblasts, suggesting the majority of bone-lining osteoblasts were of host-descent. Similar findings were observed when newly formed osteocytes were quantified (Figure 2C). Again, a dose-dependent increase was observed for both human- and rat-specific osteocytes, however, a majority of these osteocytes were indeed of host origin. These findings suggest that

PSC mediate bone formation via, primarily, a paracrine-mediated mechanism, although some PSC undergo direct differentiation.

Activation of Wnt signaling during hPSC Osteogenic Differentiation

Next, we sought to investigate the process of human PSC osteogenic differentiation and its correlate with changes in Wnt signaling over time. As anticipated, when hPSC were cultured in osteogenic medium, a steady and significant increase was observed in osteogenic markers, Osteocalcin (OCN) and master osteogenic factor, Runt-related transcription factor 2 (Runx2) (Figure 3A). Expression of gene markers associated with Wnt signaling was observed to increase early in osteogenic differentiation with *Axin2* and *cMYC* peaking on days 6 and 3, respectively (Figure 3B). The nuclear accumulation of β-catenin, however, steadily increased throughout the observation period with a statistically significant increase noted as early as day 1 (Figure 3C). In aggregate, these data suggest that PSC, under osteogenic conditions, demonstrate increased expression of pro-osteogenic molecules and that these changes are at least partially due to Wnt signaling, during early differentiation.

WISP-1 and Wnt16 transcripts are upregulated in PSC

Next RNA Sequencing (RNASeq) was next performed to compare transcript expression levels between PSC and unpurified SVF. Four SVF and PSC populations, collected from the same four patient samples, were prepared for RNASeq analysis freshly after isolation. Focus was placed on secreted molecules, known to be associated with Wnt signaling associated genes. It was observed that WNT1-inducible-signaling pathway protein (WISP)-1 and Wnt16 were upregulated

in PSC by 72.0 fold and 21.0 fold, respectively. As such, these two molecules were subjects of future study to investigate their role in the mechanism of PSC-mediate osteogenesis.

Role of WISP-1 in PSC osteogenesis

To evaluate the role of WISP-1 on PSC osteogenesis, both gain-of-function and loss-of-function assays were performed. First, WISP-1 overexpression was assayed by two modalities: 1] plasmid overexpression of WISP-1 (Figure 4A-C) and 2] supplementation with recombinant WISP-1 protein(Figure 4D-F). Plasmid success was assessed by qRT-PCR, and it was observed that PSC, transfected with the WISP-1 plasmid, possessed a 11.9-fold increase WISP-1 expression (Figure 4A). In PSC transfected with this plasmid, an increase was observed in osteogenic markers *RUNX2* and *OCN* (Figure 4B,C). Further, in hPSC treated with recombinant WISP-1, an increase in *RUNX2* and *OCN* expression was also observed (Figure 4D,E). Previous studies have demonstrated that WISP-1 is a potent inhibitor of SOST (an inhibitor of both the Wnt canonical pathway and BMP-2 pathway)[57, 58]. SOST operates by binding and inhibiting BMP2 signal transduction[59], and by binding to LRP5/6, inhibiting canonical Wnt signaling[57]. Therefore, the upregulation of WISP-1 was hypothesized to potentiate osteogenesis by promoting two major osteogenic signal transduction pathways: 1] canonical Wnt pathway and 2] BMP-2 pathway. To evaluate the effect on the BMP-2 signaling, PSC were co-treated with WISP-1 and BMP2. As hypothesized, a synergistic increase in *ALP* (alkaline phosphatase) expression was observed (Figure 4F).

Next, to investigate the necessity of *WISP-1* on the osteogenic potential of PSC, *WISP-1* was knocked down utilizing *WISP-1 siRNA*. A single siRNA sequence was selected that provided >90% gene silencing of WISP-1 in human PSC, assessed by qRT-PCR (Figure 5A). This

knockdown of *WISP-1* significantly decreased markers of osteogenesis in PSC, as observed by a 58% decrease in *RUNX2* transcripts levels at 3 days post-KO (Figure 5B). Similarly, with *WISP-1* knockout, the expression of alkaline phosphatase (ALP), a glycoprotein found on the surface of osteoblasts, which reflects bone metabolism, was significantly decreased (40% decrease) (Figure 5C). Additionally, alizarin red and alkaline phosphatase staining, both markers for osteogenesis, were observed to be markedly decreased when PSC were treated with *WISP-1* siRNA (Figure 5D). Lastly, we sought to evaluate the effect of recombinant BMP-2 protein on PSC treated with *WISP-1* siRNA (Figure 5E,F). Although BMP-2 protein did slightly improve *RUNX2* and *ALP* expression in WISP-1 knockout cells, this increase was modest compared to wildtype PSC, treated with BMP2 only. These data that *WISP-1* knockdown significantly inhibits osteogenic marker expression, as confirmed by a decrease in *RUNX2* and *ALP,* via indirect activation of SOST.

Taken together, WISP-1 is a critical secretory molecule that facilitates the osteogenic potential of PSC via activation of the canonical Wnt and BMP signaling pathways, through the inhibition of SOST. Loss of function studies reveal that WISP-1 silencing inhibits bone formation, while overexpression of WISP-1 activates osteogenesis.

Role of WNT16 in PSC osteogenesis

As Wnt16 was upregulated by 21-fold in PSC, when compared to SVF, the role of Wnt16 in PSC osteogenesis was next evaluated. When *WNT16* levels were assessed after PSC were cultured in osteogenic differentiation medium, it was observed that *WNT16* expression significantly increased by day 3, and steadily decreased back to baseline by day 9 (Figure 6A), suggesting *WNT16* plays a role in early osteogenic differentiation. Previous studies have established WNT16 as a known a mixed canonical and noncanonical ligand suggesting that it

conditionally activates two separate signal transduction cascades. Moreover, Ozeki *et al* reported that BMP-2 promotes WNT16 binding to the Fzd2/LRP5 pathway, further activating the canonical pathway via accumulation of cellular β-catenin[60]. Herein, we observed an early activation of the canonical pathway with Wnt16 treatment, followed by an inactivation of the canonical pathway and activation of the non-canonical pathway. When PSC were co-cultured with recombinant WNT16, an early increase in the markers of the canonical Wnt pathway (*AXIN2* and *cMYC*) was observed at day 3(Figure 6B). However, beginning on day 6, these levels were significantly decreased compared to control suggesting inhibition of the canonical Wnt pathway. This was paralleled with an increase in osteogenic markers *RUNX2*, *ALP*, and *OCN*, suggesting activation of the noncanonical pathway and promotion of osteogenic differentiation (Figure 6C). Moreover, there was a significant increase in bone nodule formation when PSC were cultured with recombinant WNT16 protein (Figure 6D). This increase in osteogenic differentiation was accompanied by an increase of noncanonical signaling molecule, JNK activity in WNT16-treated PSC, as shown by p46 and p54 phosphorylation assessed by western blot (Figure 6E).

To further confirm the importance of WNT16 in the osteogenic effect of PSC, knockdown was performed using *WNT16* siRNA (Figure 7). qRT-PCR confirmed the knockdown efficiency of WNT16 mRNA at 60% (Figure 7A). This decrease in Wnt16 expression was correlated with a significant decrease in osteogenic markers RUNX2, ALP and OCN by 43%, 60% and 60%, respectively (Figure 7B). Further examination by ALP and AR staining confirmed reduced osteogenic differentiation with *WNT16* siRNA (Figures 7C,D). ALP staining was reduced by 64.1% (Figure 7C), while bone nodule deposition as examined by AR staining was reduced by 70.0% (Figure 7D). These data suggest that Wnt16 plays an important role in the commitment and

differentiation of PSC down the osteogenic lineage, and is necessary for PSC to elicit their osteogenic effect.

Discussion

As previously mentioned the number of orthopaedic procedures performed per annum is steadily increasing however the gold standard of treatment, autologous bone grafting, has remained stagnant. Unfortunately, there exists a number of drawbacks in the use of autologous bone grafting, including donor site morbidity, increased risk of infection, limited supply, and increased intraoperative time. With the utilization of PSC, we can dramatically decrease the surgical time by ease of isolation and purification, and the donor site morbidity due to the relative ease of the liposuction procedure. Until present, the modality by which PSC induced bone formation, however, remained unclear. Herein, we demonstrated that PSC primarily induce bone via paracrine-mediated recruitment and induction of local osteoprogenitor, mesenchymal stem cells. This recruitment and differentiation is due to secretory Wnt-related molecules, of which WISP-1 and Wnt16 were significantly upregulated in PSC compared to their unpurified stromal vascular fraction. Upregulation of WISP-1 and Wnt16 in PSC induced improved bone formation, whereby, inactivation demonstrated a significant decrease in osteogenic potential. This osteogenic differentiation was due to activation of both the BMP pathway, as well as the Wnt β-catenin pathways (schematized in Figure 8).

Previous studies have confirmed the role of WISP-1 in both BMP-2 and Wnt canonical pathways. As a member of the CCN (connective tissue growth factor, Cyr61, NOV) family of growth factors, WISP-1 is involved in skeletogenesis and bone healing[61]. In a fracture repair

model, WISP-1 expression has been observed to increase, spatiotemporally, recapitulating skeletal development[62]. Within BMP-2 signaling, WISP-1 serves two roles. First, it serves as a potent inhibitor of SOST[57, 58], a protein that competes with BMP receptors for BMP-2 binding[63]. Therefore, by increasing the amount of readily available BMP-2 to bind to the BMP receptors by binding and inhibiting SOST, WISP-1 promotes BMP signaling. Second, WISP-1 has been shown to potentiate BMP signaling by binding directly to BMP-2 and increasing its osteogenic effect, in a dose-dependent manner[64]. Therefore by means of this dual-effect of WISP-1, there is a net increase in the amount of BMP-2 available, and the available BMP-2 can functionally interact with WISP-1, enhancing the efficacy of BMP-2.

WISP-1 also plays a role in the activation of the canonical Wnt pathway. WISP-1, as previously mentioned, binds to SOST[57, 58] which is an inhibitor of the canonical Wnt pathway[65]. By binding to the extracellular domain of Wnt co-receptors LRP5 and LRP6, SOST disrupts the interaction between the Wnt-induced Frizzled (Fzd) and LRP complex and therefore attenuates canonical Wnt signaling[65]. Thus, an inactivation of SOST via binding of WISP-1, results in the interaction of Fzd and LRP proteins subsequent to Wnt ligand binding, and ultimately accumulation of nuclear β-catenin resulting in osteogenic differentiation[66]. In aggregate, WISP-1 plays several roles in the osteogenic effect of PSC. By simulating natural skeletogenesis as a member of the CCN family, WISP-1 promotes BMP-2 signaling and inactivates SOST, thereby un-inhibiting the BMP-2 and canonical Wnt pathways.

As a generally accepted mixed canonical and noncanonical Wnt ligand, WNT16 plays a complex role in the osteogenic differentiation of PSC[67]. First, as a canonical ligand, previous authors demonstrated that in WNT16-deficient mice, a decrease in periosteal bone formation and mineral apposition was observed. These findings are in conjunction with a significant decrease in

canonical markers β-catenin and Axin2, but not noncanonical markers Nfatc1, Tnnt2, and JNK[68]. Conversely, other authors have reported that Wnt16 serves as a protector from over activation of the canonical pathway, thereby supporting homeostasis. In a study by Nalesso, *et al.* WNT16 reduced the capacity of WNT3A, potent canonical-activator, to activate the canonical WNT pathway[69]. Herein, we observe both phenomenon. Early treatment with WNT16 resulted in a statistically significant increase in canonical marker, AXIN2, however, this expression decreased by day 6 (*see again* Figure 6B). Furthermore, we observed that WNT16 treatment resulted in an increase in downstream noncanonical protein, JNK, over time. Therefore, contingent on previous studies and the data herein, there exists a high dependence on the model system and culture conditions on the role of Wnt16. Nonetheless, it plays a critical role, in conjunction with WISP-1 in the commitment of mesenchymal stem cell down the osteogenic fate and a paramount role in PSC-mediated osteogenic differentiation.

Conclusion & Future Direction

Our findings partially elucidate the mechanism whereby perivascular stem cells induce their robust osteogenic effect. We have resolved that human PSC operate via a primarily paracrine-mediated mechanism, although some direct differentiation does indeed occur. By means of RNASeq, WISP-1 and Wnt16 were discovered to be upregulated secretory, Wnt-relatated, molecules in PSC. Upon further investigation, their roles were understood in activation of the osteogenic pathway of BMP-2, as well as both the canonical and noncanonical Wnt pathways. In aggregate, both WISP-1 and WNT16 were confirmed to play an important and necessary role in the commitment and differentiation of PSC down an osteogenic lineage.

Future studies should not only further investigate the mechanism of hPSC, however, should expand upon optimizing their isolation protocol. Although FACS is far superior in comparison to culture, in respect to speed and efficacy of isolation, recently investigators have utilized magnetics via MACS (magnetic activated cell sorting) to isolate mesenchymal stem cells with success[70]. Therefore, moving forward, studies should be performed to both understand the mechanism of hPSC, improving their isolation, and confirming their safety profile to begin translation into the clinical setting.

Materials & Methods

Immunohistochemistry of Rat Spinal Fusion Samples

After spines were harvested from previous study[56], samples were decalcified using 19% EDTA and embedded in paraffin. Immunohistochemical staining was performed with primary antibodies against both human and rat major histocompatibility complex (MHC) class I antigens (Santa Cruz Biotechnology using the ABC (Vector Laboratories, Burlingame, CA, http://www.vectorlabs.com) method. Immunohistochemistry was performed after paraffin slices were deparaffinized, dehydrated, rinsed, and incubated with 3% H_2O_2 for 20 minutes. All sections were then blocked with 0.1% bovine serum albumin in PBS for 1 hour. At a dilution of 1:100, primary antibodies were added to each section and incubated at 37°C for 1 hour or overnight at 4°C. Images were obtained on an Olympus (Center Valley, PA, http://www.olympusamerica.com) BX51 fluorescence microscope. Species specific osteoblast and osteocyte quantifications were performed for positive staining of MHC at 40x magnification using Photoshop (Adobe Systems Inc., San Jose, CA, http://www.adobe.com).

PSC Isolation

PSC were isolated from human subcutaneous adipose tissue via FACS. Lipoaspirate was stored for no more than 48 h at 4°C before processing. Subsequently, collagenase digestion was performed, yielding the human SVF (stromal vascular fraction. Briefly, lipoaspirate was diluted with an equal volume of phosphate-buffered saline (PBS) before digestion with Dulbecco's modified Eagle's medium (DMEM) containing 3.5% bovine serum albumin (Sigma-Aldrich, St. Louis, MO) and 1 mg/mL type II collagenase for 70 min under agitation at 37°C. Adipocytes were next separated and removed by centrifugation. The pellet was then resuspended in red cell lysis buffer (155 mM NH4Cl, 10 mM KHCO3, and 0.1 mM EDTA) and incubated for 10 min at room temperature. After centrifugation, pellets were again resuspended in PBS and filtered at 70 mm. The resulting hSVF was further processed for cell sorting (to isolate PSC). A subset of this SVF was shipped for RNA Sequencing with patient-matched PSC. hSVF was incubated with a mixture of the following directly conjugated antibodies: anti-CD34- phycoerythrin (1:100; Dako, Glostrup, Denmark), anti- CD45-allophycocyanin (1:100; Santa Cruz Biotechnology, Inc., Santa Cruz, CA), and anti-CD146-fluorescein isothiocyanate (1:100; AbD Serotec, Raleigh, NC). All incubations were performed at 4°C for 15min in the dark. Before sorting, 4',6-diamidino-2-phenylindole (DAPI; 1:1000; Invitrogen, Carlsbad, CA) was added for dead cell exclusion; the solution was then passed through a 70-mm cell filter and then run on FACSAria cell sorter (BD Bio- sciences, San Diego, CA). Sorted cells were plated for *in vitro* studies. In this manner, distinct microvessel pericytes (CD34-, CD146+, and CD45-) and adventitial cells (CD34+, CD146-, and CD45-) were isolated and combined to constitute the PSC population. Cells were cultured at 37°C in a

humidified atmosphere. The expansion of cells was performed in DMEM, 20% fetal bovine serum (FBS), and 1% penicillin/streptomycin. Medium was changed every 3 days.

RNA Sequencing

Patient matched samples of SVF and purified PSC were next isolated to single cell lysates in 96-well plates. Plates were stored at -80°C and shipped to Fluidigm Corporation (South San Francisco) on dry ice for RNASeq to be performed[71], on patient-matched SVF and PSC samples. Transcripts of interest were secreted, Wnt-related molecules.

Assays performed in growth medium

PSC were seeded in six-well plates at a density of $1x10^5$ cells/well and allowed to adhere overnight. Cells were cultured in DMEM +10% FBS +1% penicillin/ streptomycin and treated with recombinant WISP-1 (200ng/mL), BMP-2 (50ng/mL), or WNT16 (50ng/mL) for 6 days, at which time RNA isolation was performed.

Osteogenic differentiation assays

Assays for PSC differentiation were adapted from prior publications[72-74]. The osteogenic differentiation medium (ODM) was constituted with 10mM β-glycerophosphate and 50 mM ascorbic acid in DMEM +20% FBS. Medium supplemented with Wnt ligand was changed q3d of differentiation.

Alkaline phosphatase (ALP) staining was performed using the leukocyte alkaline phosphatase kit (Sigma- Aldrich). In brief, cells were seeded in 24-well plates (density of $1x10^4$ cells/well). Cells were cultured under osteogenic differentiation conditions for 12 days prior to

staining. Cells were then washed with PBS and fixed with formalin for 10min. Following fixation, cells were stained using leukocyte alkaline phosphatase kit (Sigma-Aldrich) according to the manufacturer's protocol. Cells were incubated in ALP stain for 15 min at 37°C and subsequently washed with PBS. Cells were allowed to dry and pictures were taken at 100x magnification using the Olympus IX71 inverted system microscope (Olympus, Cypress, CA). Relative staining was quantified using Adobe Photoshop CC2015.

For the detection of mineralization, cells were seeded in growth medium in 24-well plates (density of $1x10^4$ cells/well). After cell seeding for twenty-four hours, the basal medium was replaced with ODM containing WISP-1 or WNT16 in triplicate for 12 days (200ng/mL or 50ng/mL, respectively). Cells were washed with PBS and fixed with 4% paraformaldehyde. Subsequent to fixation, cells were stained with 2% alizarin red (Sigma-Aldrich) at room temperature for 15 min, washed with deionized water, and allowed to dry. Photographs were taken at 100x magnification using the Olympus IX71 inverted system microscope (Olympus). To quantify bone nodule deposition, 10% v/v acetic acid was added and cells were incubated at room temperature for 30 min while shaking. Cells were then scraped from the wells and vortexed for 30s. Next, cells were overlaid with mineral oil and heated to 85°C for 10 min. Cells were briefly cooled on ice for 5 min and then centrifuged at 20,000 g for 15 min. Ten percent ammonium hydroxide was added to adjust the pH to between 4.1 and 4.15. Absorbance was measured in triplicate at 405nm in 96-well plates using Epoch microspectrophotometer (Bio-Tek, Winooski, VT).

RNA Isolation and qRT-PCR

Gene expression was assayed by quantitative real-time polymerase chain reaction (RT-PCR), based on previous publications[72, 74, 75]. Time points for specific gene expression include 3, 6, 9, and 12 days of osteogenic differentiation. In brief, total RNA was extracted using the RNeasy Kit (Qiagen, Santa Clarita, CA). One microgram of total RNA from each sample was subjected to first-strand complementary deoxyribonucleic acid (cDNA) synthesis using the SuperScript III Reverse-Transcriptase Kit (Life Technologies) to a final volume of 20 mL The reverse transcription reaction was performed at 65°C for 5 min, followed by 50°C for 50 min and 85°C for 5 min. For qRT-PCR, the reactions were performed using 2xSYBR green RT-PCR master mix and an ABI PRISM 7300 qRT-PCR system instrument (Applied Biosystems, Foster City, CA). qRT-PCR was performed using 96-well optical plates at 95°C for 10 min, followed by 40 cycles at 95°C for 15 s and at 60°C for 60 s. The relative quantification of gene expression was performed using a Comparative CT method according to the manufacturer's protocol and was normalized to the expression levels of the housekeeping gene, GAPDH or ACTB, in each sample.

Whole Protein Extraction and Western Blot Analysis

Protein extraction and western blot analysis were adapted from our prior publications[72, 74]. Western blot analysis was performed using antibodies against nuclear β-catenin, JNK (1:1000, Cell Signaling Technologies, Danvers. MA), GAPDH, or H3 (Santa Cruz Biotechnology). To measure cytoplasmic and nuclear β-catenin protein levels, cells were seeded in six-well plates at a density of $4x10^4$ cells/well. After attachment, basal medium was replaced with starvation medium containing DMEM + 1% FBS for 16 h. Medium was then replaced with ODM for up to 12 days. Cells were then washed with PBS and re- suspended in 150 mL of radioimmunoprecipitation assay

buffer (RIPA) (Thermo Fisher Scientific) with 100· Halt protease/phosphatase inhibitor cocktail (Life Technologies) added. Nuclear and cytoplasmic protein was isolated using the NE-PER Nuclear and Cytoplasmic Extraction Kit (Thermo Fisher Scientific).

JNK quantifications were performed by initially seeding cells in six-well plates at a density of $4x10^4$ cells/well. After attachment, basal medium was replaced with starvation medium containing DMEM + 1% FBS for 16h. Cells were then treated with WNT16 for 15, 30, 60, and 120 min in starvation medium and were resuspended in 150 mL of RIPA buffer (Thermo Fisher Scientific) with Halt protease/phos- phatase inhibitor cocktail (Life Technologies) added. For western blot analysis, 30 mg of total protein combined with 5· reducing loading buffer (Thermo Fisher Scientific) was boiled for 5 min, separated by SDS-PAGE, and electrotransferred to a nitrocellulose membrane (GE Healthcare, Piscataway, NJ) at 200 V for 1 h at 4°C. The membrane was blocked for 1 h in Superblock (TBS) Blocking Buffer (nuclear β-catenin, cytoplasmic β-catenin, ACTB, GAPDH, nuclear H3) (Thermo Fisher Scientific) or 5% BSA (JNK).

Western blot analysis was performed using antibodies against nuclear β-catenin (Cell Signaling Technologies), GAPDH (Santa Cruz Biotechnology), H3, or JNK(Cell Signaling Technologies) at dilutions of 1:1000 over- night at 4°C, then washed with TBST, and incubated in a secondary antibody (Abcam, Cambridge, MA) at 1:10,000 dilution in blocking buffer at room temperature for 1h. Following incubation, the membranes were washed three times with TBST and proteins were visualized using the Peirce enhanced chemiluminescence western blotting substrate (Thermo Fisher Scientific) as per the manufacturer's instructions. Quantitation of western blot intensity was performed using NIH ImageJ.

Small interfering RNA and transfection

Knockdown of *WISP-1* and *WNT16* were performed using Silencer Select chemically synthesized small interfering RNA (siRNA) (Thermo Fisher Scientific). Cells were seeded in six-well plates (density of $4x10^4$). At 50% confluence, basal medium was replaced with antibiotic-free basal medium. Transfection was performed using X-tremeGENE siRNA Transfection Reagent (Sigma-Aldrich) and 150 pM *WISP*-1 siRNA, 150 pM *WNT16* siRNA or scrambled siRNA diluted in minimal essential medium (Opti-MEM). For the confirmation of siRNA efficiency, six hours after transfection, medium was replaced with basal medium and the efficiency of the knockdown was validated using qRT-PCR. For alizarin red (AR) and ALP staining, six hours after transfection, medium was replaced with ODM and cells were cultured under osteogenic differentiation conditions for 12 days.

Statistical analysis.

All results are expressed as mean–standard deviation (SD). Statistical analyses were performed using the SPSS16.0 software. Normal quantile plots were examined to confirm the data followed the normal Gaussian distribution, allowing the use of parametric methods. Student's t test was used for two-group comparisons, and one-way ANOVA test was used for comparisons of three or more groups, followed by Tukey's post hoc test. Differences were considered significant when $p < 0.05$.

Figures

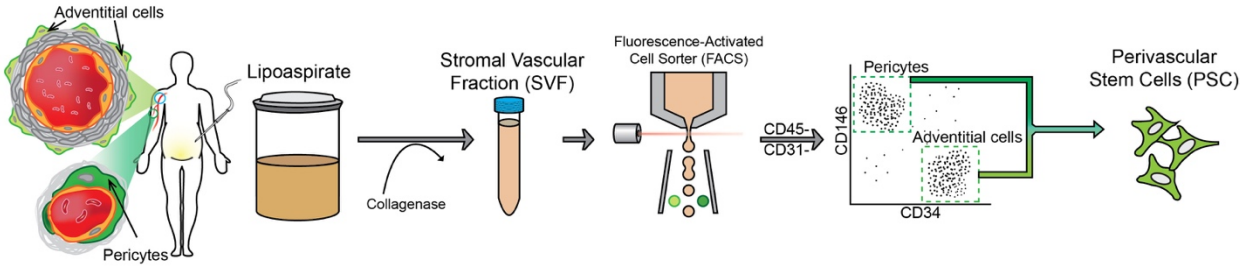

Figure 1. Isolation Protocol of PSC. Perivascular stem cells (PSC) are comprised of two distinct MSC populations, consisting of pericytes which are found on the periphery of microvessels and adventitial cells which are found on larger vessels. Subsequent to liposuction procedure, a lipoaspirate is collected and treated with collagenase. This collagenase-treated sample yields the stromal vascular fraction (SVF). To purify PSC, SVF is sorted for negative expression of CD45, CD31, and differential expression of CD146 and CD34.

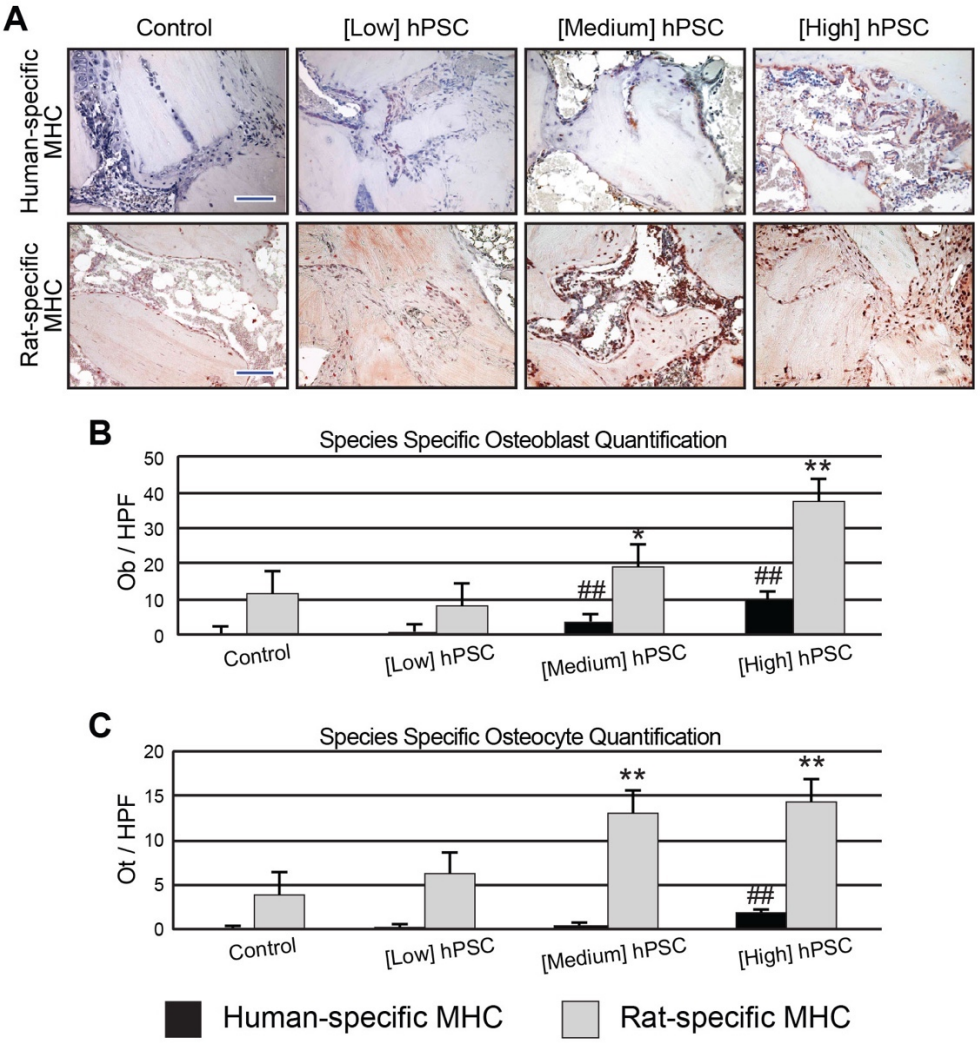

Figure 2. Osteoprogenitor origin of newly formed bone cells. (A) Immunohistochemistry was performed against human and rat MHC on samples of rat vertebrae treated with increasing dosages of human PSC. Quantifications were performed at 40x magnification for quantity of species-specific **(B)** osteoblasts and **(C)** osteocytes per high powered field. *Abbreviations*: hMHC, human-specific major histocompatibility complex; HPF, higher power field; hPSC, human perivascular stem cells; MHC, major histocompatibility complex; Ob, osteoblasts; Ot, osteocytes; rMHC, rat-specific major histocompatibility complex. *p≤0.05 compared to with rat-specific control values, **p≤0.01 compared to with rat-specific control values, ##p≤0.01 compared to human-specific control values. Adapted from Chung *et al*[56], with permission.

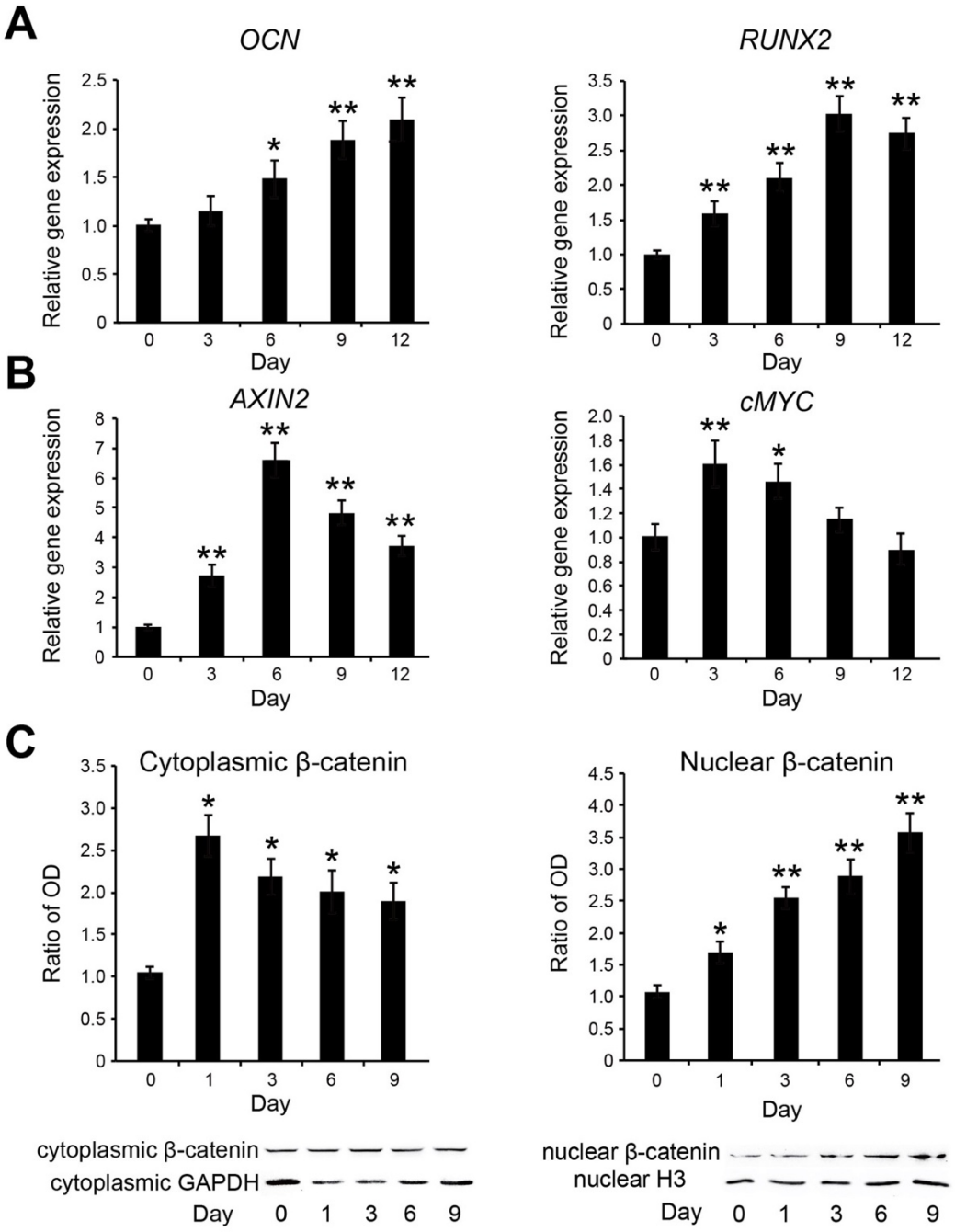

Figure 3. Regulation of Wnt signaling during hPSC osteogenic differentiation. (A) mRNA transcript levels of hPSC osteogenic markers *OCN* and *RUNX2* were calculated over 12 days. **(B)** Canonical Wnt-related transcript levels increased early during osteogenic differentiation and began decreasing after day 6. **(C)** Intracellular β-catenin was next quantified and cytoplasmic β-catenin spiked at day 1 and began decreasing as nuclear β-catenin consistently increased, consistent with activation of the canonical Wnt pathway. *Abbreviations*: OCN, Osteocalcin; RUNX2, Runt Related Transcription Factor 2. *p≤0.05 compared to respective control. **p≤0.01 compared to respective control. Adapted from Shen *et al*[74], with permission.

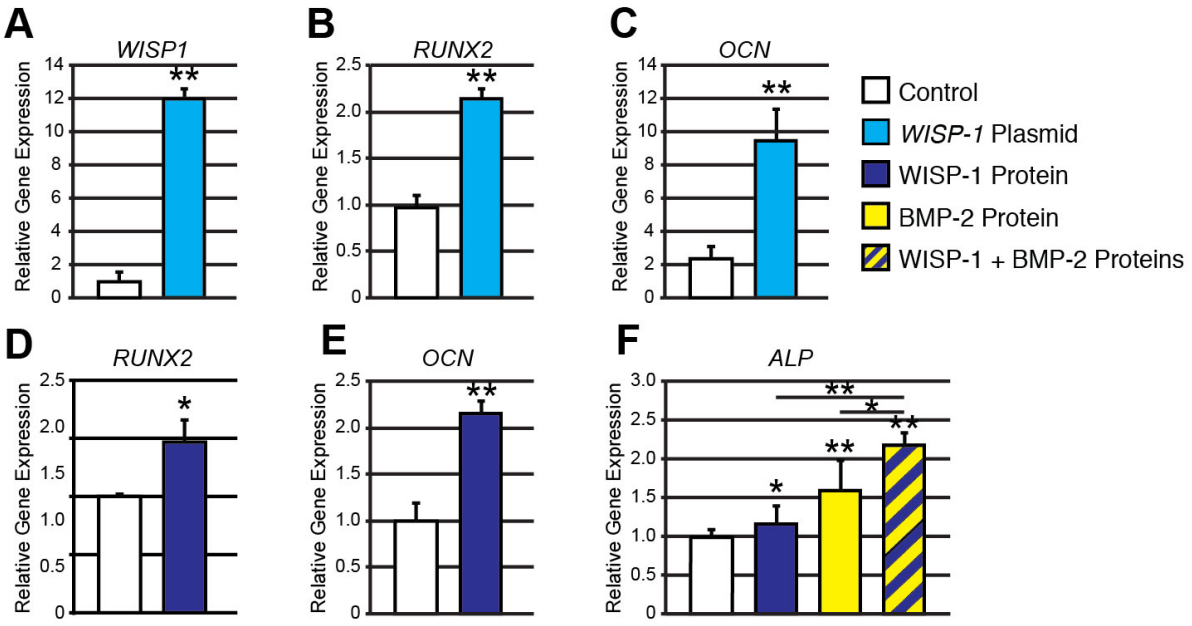

Figure 4. WISP-1 upregulation increases osteogenic differentiation. The effect WISP-1 overexpression by either **(A-C)** plasmid or **(D-F)** recombinant protein was next assessed. **(A)** Plasmid transfection demonstrated a near 12-fold increase in *WISP-1* expression. This increase in *WISP-1* expression was correlated with a significant increase in expression of osteogenic markers **(B)** *RUNX2* and **(C)** *OCN*. **(D,E)** Further, when PSC were treated with recombinant WISP-1 protein, an increase in *RUNX2* and *OCN* expression was observed. **(F)** Individual treatment with WISP-1 and BMP-2 both increased ALP staining, however co-administration demonstrated a statistically significant and synergistic increase on ALP expression. *Abbreviations*: WISP-1, WNT1 Inducible Signaling Pathway Protein 1; RUNX2, Runt Related Transcription Factor 2; OCN, Osteocalcin. ALP, Alkaline Phosphatase. BMP, Bone Morphogenetic Protein. *p≤0.05 compared to respective control. **p≤0.05 compared to respective control.

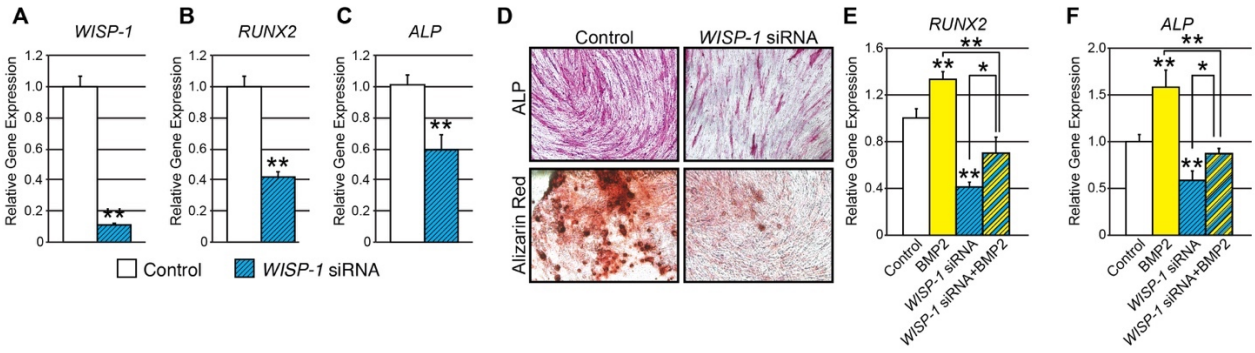

Figure 5. *WISP-1* downregulation inhibits osteogenic differentiation. siRNA was constructed against *WISP-1*. **(A)** Knockdown was confirmed with >90% gene silencing of WISP-1. This downregulation was coincident with a decrease in osteogenic markers **(B)** *RUNX2* and **(C)** *ALP*. **(D)** ALP and Alizarin red staining of bone nodules showed a decrease stain intensity in *WISP-1* knockdown samples. **(E,F)** Osteogenic markers, *RUNX2* and *ALP*, expression was next evaluated. Supplementation with BMP2 increased *RUNX2* and *ALP* expression, while *WISP-1* siRNA inhibited expression. The osteogenic effect of BMP2 was inhibited when cells we co-exposed to BMP2 and *WISP-1* siRNA. *Abbreviations*: WISP-1, WNT1 Inducible Signaling Pathway Protein 1; RUNX2, Runt Related Transcription Factor 2; ALP, Alkaline Phosphatase, BMP2, Bone Morphogenetic Protein 2; siRNA, small interfering ribonucleic acid. *$p \leq 0.05$ compared to respective control. **$p \leq 0.01$ compared to respective control. Adapted from Shen *et al*[74], with permission.

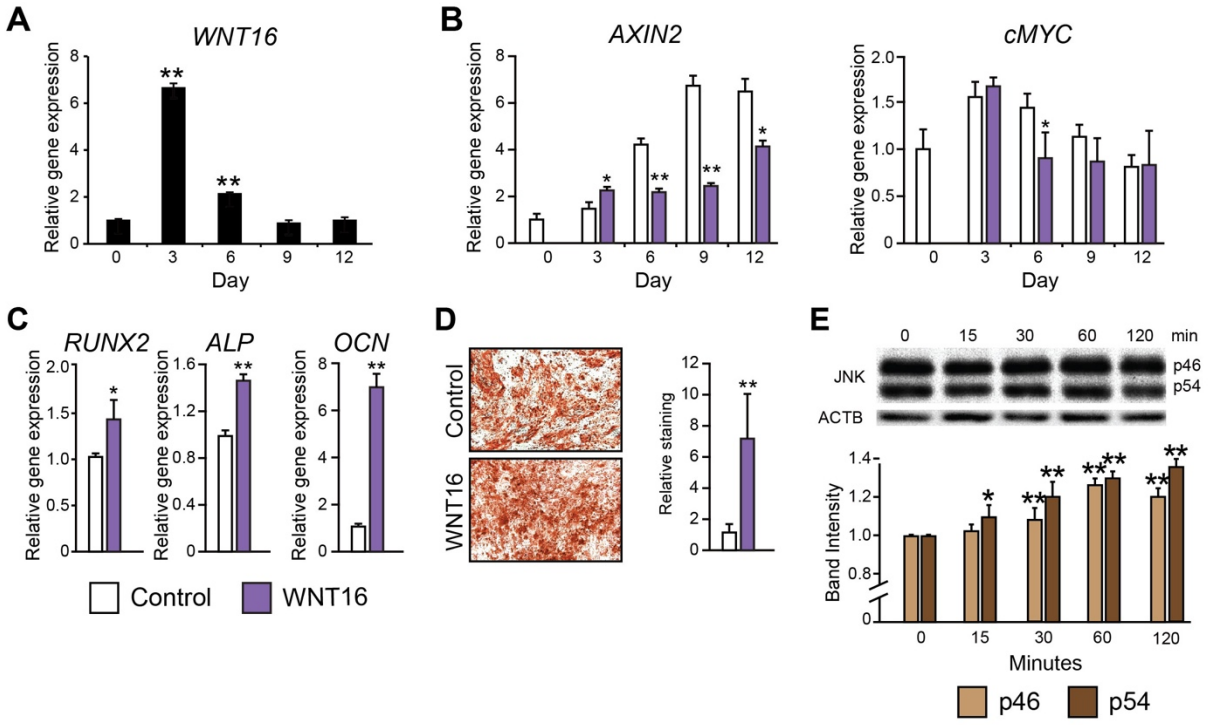

Figure 6. WNT16 and Wnt signaling. (A) hPSC cultured in osteogenic differentiation medium demonstrate a significant increase in *WNT16* early during osteogenic differentiation which significantly and steadily decreases after day 3. **(B)** hPSC treated with recombinant WNT16 protein demonstrate an early increase in canonical Wnt signaling transcripts *AXIN2* and *cMYC* which decreased demonstrating an early activation and subsequent inactivation of the canonical Wnt pathway. **(C)** Osteogenic markers *RUNX2*, *ALP*, and *OCN* were quantified using qRT-PCR and demonstrated a significant increase when hPSC were treated with recombinant WNT16 protein. **(D)** Bone nodule formation in hPSC were next stained with Alizarin red and quantified for stain intensity. **(E)** Western blots and densiometry demonstrated that with Wnt16 treatment, a steady and significant increase in noncanonical JNK was observed. *Abbreviations*: RUNX2, Runt Related Transcription Factor 2; ALP, Alkaline Phosphatase; OCN, Osteocalcin; AR, Alizarin Red; JNK, Jun N-terminal Kinase; ACTB, Actin beta; qRT-PCR, Quantitative Real Time Polymerase Chain Reaction. *p≤0.05 compared to respective control. **p≤0.01 compared to respective control. Adapted from Shen *et al*[74], with permission.

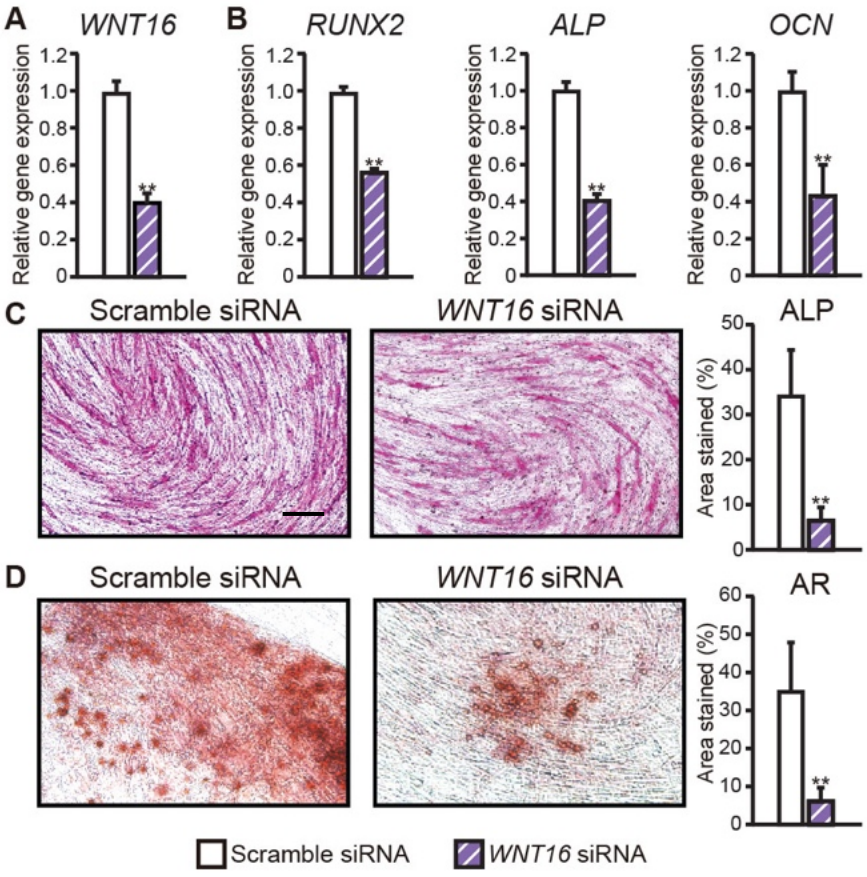

Figure 7. WNT16 downregulation inhibits osteogenic differentiation. (A) *Wnt16* siRNA was successfully utilized to knockdown *WNT16* expression (60% decrease in expression confirmed by qRT-PCR. **(B)** This decrease in *WNT16* resulted in decrease in osteogenic markers *RUNX2*, *ALP*, and *OCN* at 3 days post-transfection. **(C)** ALP staining was performed at 12 days after transfection and a significant decrease in staining intensity was observed. **(D)** AR staining performed on bone nodule deposition was subsequently quantified and a reduction was observed in *WNT16* siRNA-treated cells. *Abbreviations*: RUNX2, Runt Related Transcription Factor 2; ALP, Alkaline Phosphatase; OCN, Osteocalcin; AR, Alizarin Red; siRNA, small interfering ribonucleic acid; qRT-PCR, Quantitative Real Time Polymerase Chain Reaction. Black scale bar = 200 μm **p≤0.01 compared to respective control. Adapted from Shen et al[74], with permission.

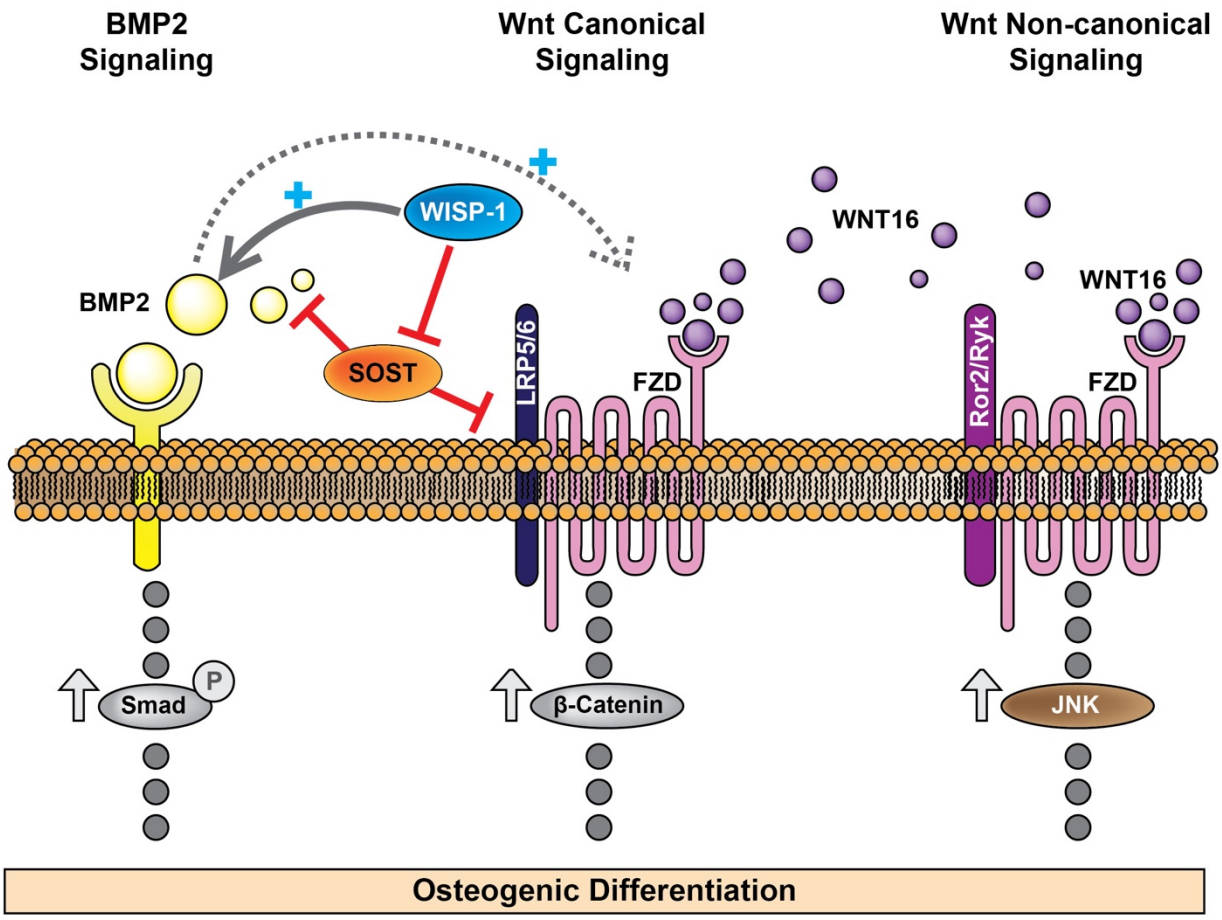

Figure 8. Schematic representation of the hypothesized role of WNT16 & WISP-1 in PSC osteogenic differentiation.

Works Cited

[1] Giannoudis PV, Dinopoulos H, Tsiridis E: Bone substitutes: an update. Injury 2005, 36 Suppl 3:S20-7.

[2] Bagaria V, Prasada V: Bone morphogenic protein: Current state of field and the road ahead. JOrthopaedics, 2005. p. e3.

[3] Sakkas A, Wilde F, Heufelder M, Winter K, Schramm A: Autogenous bone grafts in oral implantology-is it still a "gold standard"? A consecutive review of 279 patients with 456 clinical procedures. Int J Implant Dent 2017, 3:23.

[4] Mikhael MM, Huddleston PM, Nassr A: Postoperative culture positive surgical site infections after the use of irradiated allograft, nonirradiated allograft, or autograft for spinal fusion. Spine 2009, 34:2466-8.

[5] Sawin PD, Traynelis VC, Menezes AH: A comparative analysis of fusion rates and donor-site morbidity for autogeneic rib and iliac crest bone grafts in posterior cervical fusions. Journal of neurosurgery 1998, 88:255-65.

[6] Wolfe SA: Complications of harvesting cranial bone grafts. Plastic and reconstructive surgery 1996, 98:567.

[7] Khan SN, Lane JM: The use of recombinant human bone morphogenetic protein-2 (rhBMP-2) in orthopaedic applications. Expert Opin Biol Ther 2004, 4:741-8.

[8] Boden SD, Zdeblick TA, Sandhu HS, Heim SE: The use of rhBMP-2 in interbody fusion cages. Definitive evidence of osteoinduction in humans: a preliminary report. Spine (Phila Pa 1976) 2000, 25:376-81.

[9] Walker DH, Wright NM: Bone morphogenetic proteins and spinal fusion. Neurosurg Focus 2002, 13:e3.

[10] Wong DA, Kumar A, Jatana S, Ghiselli G, Wong K: Neurologic impairment from ectopic bone in the lumbar canal: a potential complication of off-label PLIF/TLIF use of bone morphogenetic protein-2 (BMP-2). Spine J 2008, 8:1011-8.

[11] McKay B, Sandhu HS: Use of recombinant human bone morphogenetic protein-2 in spinal fusion applications. Spine (Phila Pa 1976) 2002, 27:S66-85.

[12] Joseph V, Rampersaud YR: Heterotopic bone formation with the use of rhBMP2 in posterior minimal access interbody fusion: a CT analysis. Spine (Phila Pa 1976) 2007, 32:2885-90.

[13] Shah RK, Moncayo VM, Smitson RD, Pierre-Jerome C, Terk MR: Recombinant human bone morphogenetic protein 2-induced heterotopic ossification of the retroperitoneum, psoas muscle, pelvis and abdominal wall following lumbar spinal fusion. Skeletal Radiol 2010, 39:501-4.

[14] Boraiah S, Paul O, Hawkes D, Wickham M, Lorich DG: Complications of recombinant human BMP-2 for treating complex tibial plateau fractures: a preliminary report. Clin Orthop Relat Res 2009, 467:3257-62.

[15] Chen NF, Smith ZA, Stiner E, Armin S, Sheikh H, Khoo LT: Symptomatic ectopic bone formation after off-label use of recombinant human bone morphogenetic protein-2 in transforaminal lumbar interbody fusion. J Neurosurg Spine 2010, 12:40-6.

[16] Lewandrowski KU, Nanson C, Calderon R: Vertebral osteolysis after posterior interbody lumbar fusion with recombinant human bone morphogenetic protein 2: a report of five cases. Spine J 2007, 7:609-14.

[17] Vaidya R, Sethi A, Bartol S, Jacobson M, Coe C, Craig JG: Complications in the use of rhBMP-2 in PEEK cages for interbody spinal fusions. J Spinal Disord Tech 2008, 21:557-62.

[18] Balseiro S, Nottmeier EW: Vertebral osteolysis originating from subchondral cyst end plate defects in transforaminal lumbar interbody fusion using rhBMP-2. Report of two cases. Spine J 2010, 10:e6-e10.

[19] Mannion RJ, Nowitzke AM, Wood MJ: Promoting fusion in minimally invasive lumbar interbody stabilization with low-dose bone morphogenic protein-2--but what is the cost? Spine J 2011, 11:527-33.

[20] Carter TG, Brar PS, Tolas A, Beirne OR: Off-label use of recombinant human bone morphogenetic protein-2 (rhBMP-2) for reconstruction of mandibular bone defects in humans. J Oral Maxillofac Surg 2008, 66:1417-25.

[21] Mindea SA, Shih P, Song JK: Recombinant human bone morphogenetic protein-2-induced radiculitis in elective minimally invasive transforaminal lumbar interbody fusions: a series review. Spine (Phila Pa 1976) 2009, 34:1480-4; discussion 5.

[22] Robin BN, Chaput CD, Zeitouni S, Rahm MD, Zerris VA, Sampson HW: Cytokine-mediated inflammatory reaction following posterior cervical decompression and fusion associated with recombinant human bone morphogenetic protein-2: a case study. Spine (Phila Pa 1976) 2010, 35:E1350-4.

[23] Garrett MP, Kakarla UK, Porter RW, Sonntag VK: Formation of painful seroma and edema after the use of recombinant human bone morphogenetic protein-2 in posterolateral lumbar spine fusions. Neurosurgery 2010, 66:1044-9; discussion 9.

[24] MacDonald KM, Swanstrom MM, McCarthy JJ, Nemeth BA, Guliani TA, Noonan KJ: Exaggerated inflammatory response after use of recombinant bone morphogenetic protein in recurrent unicameral bone cysts. J Pediatr Orthop 2010, 30:199-205.

[25] Cancedda R, Giannoni P, Mastrogiacomo M: A tissue engineering approach to bone repair in large animal models and in clinical practice. Biomaterials 2007, 28:4240-50.

[26] Asatrian G, Pham D, Hardy WR, James AW, Peault B: Stem cell technology for bone regeneration: current status and potential applications. Stem Cells Cloning 2015, 8:39-48.

[27] Deans RJ, Moseley AB: Mesenchymal stem cells: biology and potential clinical uses. Experimental hematology 2000, 28:875-84.

[28] Minguell JJ, Conget P, Erices A: Biology and clinical utilization of mesenchymal progenitor cells. Brazilian journal of medical and biological research = Revista brasileira de pesquisas medicas e biologicas / Sociedade Brasileira de Biofisica [et al] 2000, 33:881-7.

[29] Schwartz RE, Reyes M, Koodie L, Jiang Y, Blackstad M, Lund T, Lenvik T, Johnson S, Hu WS, Verfaillie CM: Multipotent adult progenitor cells from bone marrow differentiate into functional hepatocyte-like cells. The Journal of clinical investigation 2002, 109:1291-302.

[30] Hayashi O, Katsube Y, Hirose M, Ohgushi H, Ito H: Comparison of osteogenic ability of rat mesenchymal stem cells from bone marrow, periosteum, and adipose tissue. Calcif Tissue Int 2008, 82:238-47.

[31] Wang Z, Goh J, Das De S, Ge Z, Ouyang H, Chong JS, Low SL, Lee EH: Efficacy of bone marrow-derived stem cells in strengthening osteoporotic bone in a rabbit model. Tissue Eng 2006, 12:1753-61.

[32] Krampera M, Pizzolo G, Aprili G, Franchini M: Mesenchymal stem cells for bone, cartilage, tendon and skeletal muscle repair. Bone 2006, 39:678-83.

[33] Bonab MM, Alimoghaddam K, Talebian F, Ghaffari SH, Ghavamzadeh A, Nikbin B: Aging of mesenchymal stem cell in vitro. BMC cell biology 2006, 7:14.

[34] Izadpanah R, Trygg C, Patel B, Kriedt C, Dufour J, Gimble JM, Bunnell BA: Biologic properties of mesenchymal stem cells derived from bone marrow and adipose tissue. J Cell Biochem 2006, 99:1285-97.

[35] Izadpanah R, Kaushal D, Kriedt C, Tsien F, Patel B, Dufour J, Bunnell BA: Long-term in vitro expansion alters the biology of adult mesenchymal stem cells. Cancer research 2008, 68:4229-38.

[36] Wagner W, Horn P, Castoldi M, Diehlmann A, Bork S, Saffrich R, Benes V, Blake J, Pfister S, Eckstein V, Ho AD: Replicative senescence of mesenchymal stem cells: a continuous and organized process. PloS one 2008, 3:e2213.

[37] Zuk PA, Zhu M, Mizuno H, Huang J, Futrell JW, Katz AJ, Benhaim P, Lorenz HP, Hedrick MH: Multilineage cells from human adipose tissue: implications for cell-based therapies. Tissue engineering 2001, 7:211-28.

[38] Rehman J, Traktuev D, Li J, Merfeld-Clauss S, Temm-Grove CJ, Bovenkerk JE, Pell CL, Johnstone BH, Considine RV, March KL: Secretion of angiogenic and antiapoptotic factors by human adipose stromal cells. Circulation 2004, 109:1292-8.

[39] Traktuev DO, Merfeld-Clauss S, Li J, Kolonin M, Arap W, Pasqualini R, Johnstone BH, March KL: A population of multipotent CD34-positive adipose stromal cells share pericyte and mesenchymal surface markers, reside in a periendothelial location, and stabilize endothelial networks. Circulation research 2008, 102:77-85.

[40] Hamid AA, Idrus RB, Saim AB, Sathappan S, Chua KH: Characterization of human adipose-derived stem cells and expression of chondrogenic genes during induction of cartilage differentiation. Clinics 2012, 67:99-106.

[41] Cowan CM, Shi YY, Aalami OO, Chou YF, Mari C, Thomas R, Quarto N, Contag CH, Wu B, Longaker MT: Adipose-derived adult stromal cells heal critical-size mouse calvarial defects. Nature biotechnology 2004, 22:560-7.

[42] Levi B, James AW, Nelson ER, Vistnes D, Wu B, Lee M, Gupta A, Longaker MT: Human adipose derived stromal cells heal critical size mouse calvarial defects. PloS one 2010, 5:e11177.

[43] Cui L, Liu B, Liu G, Zhang W, Cen L, Sun J, Yin S, Liu W, Cao Y: Repair of cranial bone defects with adipose derived stem cells and coral scaffold in a canine model. Biomaterials 2007, 28:5477-86.

[44] Requicha JF, Viegas CA, Albuquerque CM, Azevedo JM, Reis RL, Gomes ME: Effect of anatomical origin and cell passage number on the stemness and osteogenic differentiation potential of canine adipose-derived stem cells. Stem cell reviews 2012, 8:1211-22.

[45] Bellotti C, Stanco D, Ragazzini S, Romagnoli L, Martella E, Lazzati S, Marchetti C, Donati D, Lucarelli E: Analysis of the karyotype of expanded human adipose-derived stem cells for bone reconstruction of the maxillo-facial region. International journal of immunopathology and pharmacology 2013, 26:3-9.

[46] Corselli M, Chen CW, Sun B, Yap S, Rubin JP, Peault B: The tunica adventitia of human arteries and veins as a source of mesenchymal stem cells. Stem cells and development 2012, 21:1299-308.

[47] Crisan M, Yap S, Casteilla L, Chen CW, Corselli M, Park TS, Andriolo G, Sun B, Zheng B, Zhang L, Norotte C, Teng PN, Traas J, Schugar R, Deasy BM, Badylak S, Buhring HJ, Giacobino JP, Lazzari L, Huard J, Peault B: A perivascular origin for mesenchymal stem cells in multiple human organs. Cell stem cell 2008, 3:301-13.

[48] Crisan M, Chen CW, Corselli M, Andriolo G, Lazzari L, Peault B: Perivascular multipotent progenitor cells in human organs. Annals of the New York Academy of Sciences 2009, 1176:118-23.

[49] Crisan M, Corselli M, Chen CW, Peault B: Multilineage stem cells in the adult: a perivascular legacy? Organogenesis 2011, 7:101-4.

[50] Crisan M, Deasy B, Gavina M, Zheng B, Huard J, Lazzari L, Peault B: Purification and long-term culture of multipotent progenitor cells affiliated with the walls of human blood vessels: myoendothelial cells and pericytes. Methods in cell biology 2008, 86:295-309.

[51] Corselli M, Chen CW, Crisan M, Lazzari L, Peault B: Perivascular ancestors of adult multipotent stem cells. Arteriosclerosis, thrombosis, and vascular biology 2010, 30:1104-9.

[52] James AW, Zara JN, Zhang X, Askarinam A, Goyal R, Chiang M, Yuan W, Chang L, Corselli M, Shen J, Pang S, Stoker D, Wu B, Ting K, Peault B, Soo C: Perivascular stem cells: a prospectively purified mesenchymal stem cell population for bone tissue engineering. Stem Cells Transl Med 2012, 1:510-9.

[53] James AW, Zara JN, Corselli M, Chiang M, Yuan W, Nguyen V, Askarinam A, Goyal R, Siu RK, Scott V, Lee M, Ting K, Peault B, Soo C: Use of human perivascular stem cells for bone regeneration. J Vis Exp 2012:e2952.

[54] Askarinam A, James AW, Zara JN, Goyal R, Corselli M, Pan A, Liang P, Chang L, Rackohn T, Stoker D, Zhang X, Ting K, Peault B, Soo C: Human perivascular stem cells

show enhanced osteogenesis and vasculogenesis with Nel-like molecule I protein. Tissue engineering Part A 2013, 19:1386-97.

[55] James AW, Zara JN, Corselli M, Askarinam A, Zhou AM, Hourfar A, Nguyen A, Megerdichian S, Asatrian G, Pang S, Stoker D, Zhang X, Wu B, Ting K, Peault B, Soo C: An abundant perivascular source of stem cells for bone tissue engineering. Stem Cells Transl Med 2012, 1:673-84.

[56] Chung CG, James AW, Asatrian G, Chang L, Nguyen A, Le K, Bayani G, Lee R, Stoker D, Pang S, Zhang X, Ting K, Peault B, Soo C: Human perivascular stem cell-based bone graft substitute induces rat spinal fusion. Stem Cells Transl Med 2015, 4:538.

[57] Maeda A, Ono M, Holmbeck K, Li L, Kilts TM, Kram V, Noonan ML, Yoshioka Y, McNerny EM, Tantillo MA, Kohn DH, Lyons KM, Robey PG, Young MF: WNT1-induced Secreted Protein-1 (WISP1), a Novel Regulator of Bone Turnover and Wnt Signaling. The Journal of biological chemistry 2015, 290:14004-18.

[58] Kondo T, Handa M, Fujimura S: [Pulmonary lymphatics in lung transplantation]. Kokyu To Junkan 1991, 39:439-43.

[59] Wu M, Chen G, Li YP: TGF-beta and BMP signaling in osteoblast, skeletal development, and bone formation, homeostasis and disease. Bone Res 2016, 4:16009.

[60] Ozeki N, Mogi M, Hase N, Hiyama T, Yamaguchi H, Kawai R, Matsumoto T, Nakata K: Bone morphogenetic protein-induced cell differentiation involves Atg7 and Wnt16 sequentially in human stem cell-derived osteoblastic cells. Exp Cell Res 2016, 347:24-41.

[61] Perbal B: NOV (nephroblastoma overexpressed) and the CCN family of genes: structural and functional issues. Mol Pathol 2001, 54:57-79.

[62] French DM, Kaul RJ, D'Souza AL, Crowley CW, Bao M, Frantz GD, Filvaroff EH, Desnoyers L: WISP-1 is an osteoblastic regulator expressed during skeletal development and fracture repair. The American journal of pathology 2004, 165:855-67.

[63] Winkler DG, Sutherland MK, Geoghegan JC, Yu C, Hayes T, Skonier JE, Shpektor D, Jonas M, Kovacevich BR, Staehling-Hampton K, Appleby M, Brunkow ME, Latham JA: Osteocyte control of bone formation via sclerostin, a novel BMP antagonist. EMBO J 2003, 22:6267-76.

[64] Ono M, Inkson CA, Kilts TM, Young MF: WISP-1/CCN4 regulates osteogenesis by enhancing BMP-2 activity. J Bone Miner Res 2011, 26:193-208.

[65] Semenov M, Tamai K, He X: SOST is a ligand for LRP5/LRP6 and a Wnt signaling inhibitor. The Journal of biological chemistry 2005, 280:26770-5.

[66] Rossini M, Gatti D, Adami S: Involvement of WNT/beta-catenin signaling in the treatment of osteoporosis. Calcif Tissue Int 2013, 93:121-32.

[67] Moverare-Skrtic S, Henning P, Liu X, Nagano K, Saito H, Borjesson AE, Sjogren K, Windahl SH, Farman H, Kindlund B, Engdahl C, Koskela A, Zhang FP, Eriksson EE, Zaman F, Hammarstedt A, Isaksson H, Bally M, Kassem A, Lindholm C, Sandberg O, Aspenberg P, Savendahl L, Feng JQ, Tuckermann J, Tuukkanen J, Poutanen M, Baron R, Lerner UH, Gori F, Ohlsson C: Osteoblast-derived WNT16 represses osteoclastogenesis and prevents cortical bone fragility fractures. Nat Med 2014, 20:1279-88.

[68] Wergedal JE, Kesavan C, Brommage R, Das S, Mohan S: Role of WNT16 in the regulation of periosteal bone formation in female mice. Endocrinology 2015, 156:1023-32.

[69] Nalesso G, Thomas BL, Sherwood JC, Yu J, Addimanda O, Eldridge SE, Thorup AS, Dale L, Schett G, Zwerina J, Eltawil N, Pitzalis C, Dell'Accio F: WNT16 antagonises excessive

canonical WNT activation and protects cartilage in osteoarthritis. Ann Rheum Dis 2017, 76:218-26.

[70] Rodrigues GM, Matos AF, Fernandes TG, Rodrigues CA, Peitz M, Haupt S, Diogo MM, Brustle O, Cabral JM: Integrated platform for production and purification of human pluripotent stem cell-derived neural precursors. Stem Cell Rev 2014, 10:151-61.

[71] Wang Z, Gerstein M, Snyder M: RNA-Seq: a revolutionary tool for transcriptomics. Nature reviews Genetics 2009, 10:57-63.

[72] James AW, Shen J, Zhang X, Asatrian G, Goyal R, Kwak JH, Jiang L, Bengs B, Culiat CT, Turner AS, Seim Iii HB, Wu BM, Lyons K, Adams JS, Ting K, Soo C: NELL-1 in the treatment of osteoporotic bone loss. Nature communications 2015, 6:7362.

[73] Lee S, Zhang X, Shen J, James AW, Chung CG, Hardy R, Li C, Girgius C, Zhang Y, Stoker D, Wang H, Wu BM, Peault B, Ting K, Soo C: Brief Report: Human Perivascular Stem Cells and Nel-Like Protein-1 Synergistically Enhance Spinal Fusion in Osteoporotic Rats. Stem Cells 2015, 33:3158-63.

[74] Shen J, Chen X, Jia H, Meyers CA, Shrestha S, Asatrian G, Ding C, Tsuei R, Zhang X, Peault B, Ting K, Soo C, James AW: Effects of WNT3A and WNT16 on the Osteogenic and Adipogenic Differentiation of Perivascular Stem/Stromal Cells. Tissue engineering Part A 2018, 24:68-80.

[75] Shen J, James AW, Zhang X, Pang S, Zara JN, Asatrian G, Chiang M, Lee M, Khadarian K, Nguyen A, Lee KS, Siu RK, Tetradis S, Ting K, Soo C: Novel Wnt Regulator NEL-Like Molecule-1 Antagonizes Adipogenesis and Augments Osteogenesis Induced by Bone Morphogenetic Protein 2. The American journal of pathology 2016, 186:419-34.